Calculation of resonant short-crested waves in deep water

Mohammed Debiane[1] and Christian Kharif[2]
[1]*Faculté de Physique, Université des Sciences et de la Technologie Houari Boumedienne, B.P. 32 El Alia, Algiers 16111, Algeria*
[2]*Institut de Recherche sur les Phénomènes Hors Equilibre, 49 rue F. Joliot-Curie, B.P. 146, F 13384 Marseille Cedex 13, France*

(Received 18 January 2009; accepted 13 May 2009; published online 18 June 2009)

Solving the problem of resonant short-crested waves is very challenging because the appearance of small divisors causes the classical perturbation methods to fail. From a numerical point of view, the case of resonant gravity short-crested waves has been studied, but as far as we know, there are very few results in the case of resonant capillary-gravity short-crested waves. In fact, to the best of our knowledge, the most related study which has been made is the one of Craig and Nicholls [SIAM J. Math. Anal. **32**, 323 (2000)] who gave existence theorems for the case where the surface tension is supposed not to be too small. There is a need for such an investigation, and the work considered herein therefore provides a calculation technique and presents new results on resonant short-crested gravity-capillary waves. We overcome the technical problems associated with small divisors by using a method derived from Whitham's variational formulation of the classical problem of short-crested waves. Whitham's method is not modified in essence, but computations are carried out and organized to obtain a method that has been applied to series of cases demonstrating the robustness and flexibility of the approach. In particular, numerical solutions corresponding to three-dimensional Wilton ripples have been obtained. Moreover, these waves are also obtained for long wave configurations. This method is able to handle the case of small or zero surface tension, including the resonant cases, and works well very near the limiting two-dimensional cases. © *2009 American Institute of Physics*. [DOI: 10.1063/1.3155513]

I. INTRODUCTION

Resonant surface capillary-gravity waves, in general, have been focused in several studies following the pioneering work of Wilton[1] who proposed a fifth-order solution, using a Stokes-type perturbation expansion to the problem of two-dimensional, symmetrical, and periodic wave. The expansion was found to fail for values of the dimensionless capillary number κ $(=K^2T/\rho g)$ equal to the reciprocals of an integer. Here g is the body acceleration, K is the wave number, and T and ρ are, respectively, the surface tension and the density of the fluid. These failures lead to computational difficulties which will pose interesting challenges. Various approaches have been derived to overcome these difficulties and which revealed that multiple solutions usually exist. The most celebrated of these are the ripples found by Wilton[1] at $\kappa=1/2$: one is capillarylike, that is to say, the wave speed decreases as the amplitude increases and the other is gravitylike with a speed that increases as the amplitude increases.

In three dimensions, the problem is less extensively studied and the theory of wave solutions is still incomplete. Due to the complexity of the equations of the general problem, most of the studies were restricted to special cases. The short-crested waves are one of the simplest classes of three-dimensional waves and are therefore among the most commonly studied. The question of the existence of capillary-gravity short-crested waves was considered by Reeder and Shinbrot[2] who produced a proof only for sufficiently small amplitudes. Even in this case, there are situations where this proof cannot be applied. Effectively, there is a set of values of the relevant parameters for which it was not possible to get a solution. Furthermore, a problem of small divisors arises if there is no surface tension and, in this case, they conjectured that all solutions are unstable, even when they exist. This failure has been discussed by Roberts[3] who attributed the problem of small divisors to the phenomenon of harmonic resonance. He computed gravity short-crested waves in deep water generated by the reflection of a two-dimensional wave train arriving at a vertical seawall at some angle of incidence θ (Fig. 1). Using perturbation theory with the assumption that the velocity, the shape, and the velocity potential of the wave all depend analytically on a small parameter, he obtained a 27th-order solution and made a detailed investigation in which he derived the main properties. He showed how these waves are subject to the phenomenon of harmonic resonance at critical values of the incident wave angle that were shown to generate zero denominators in the perturbation solution coefficients. Therefore, the perturbation series will have everywhere zero radius of convergence. Near these critical angles, the radius of convergence is very small due to the division by a number which is nearly zero, causing the coefficients at higher orders in the perturbation series to increase rapidly. Furthermore, he found that for the most cases, the resonances appear at high orders, and thus they should be dissipated through viscous damping. Roberts and Peregrine,[4] who considered the limit as both incident and reflected waves are almost parallel, found that harmonic resonances are due to the multiplelike structure of the solutions. The properties of gravity short-crested waves in water

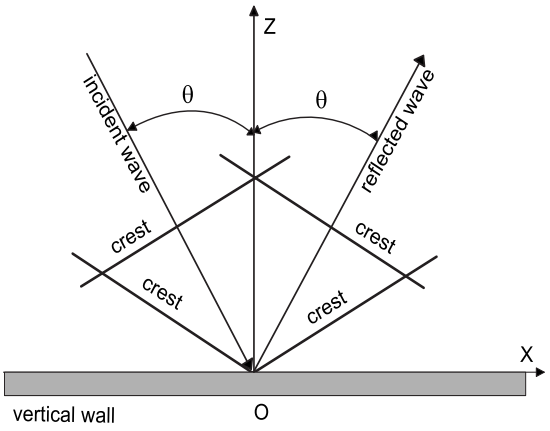

FIG. 1. Scheme of the reflection of a plane wave onto vertical wall.

of finite depth have been discussed in Marchant and Roberts[5] and, also, they found that harmonic resonance occurs for a set of values of the incident wave angle at a given depth. In the case of traveling waves without surface tension, the problem of small divisors makes the convergence of the solutions problematic. Such a situation calls into question the validity of the standard perturbation method. This requires the development of techniques other than perturbation theory to solve the problem. There has been recent progress on this problem by Iooss and Plotnikov[6] who gave, in a 119-page paper, an existence proof for waves having diamond patterns using a version of the Nash–Moser scheme. A numerical study of the stability problem associated with the harmonic resonances phenomenon has also been performed by Ioualalen and Kharif,[7] Ioualalen and Okamura,[8] and Ioualalen *et al.*[9] They showed that instabilities are weak and occur as sporadic bubbles of instability

The small divisor problems become less difficult when we consider capillary-gravity three-dimensional waves instead of pure gravity three-dimensional waves. A rigorous proof of such waves was obtained by Craig and Nicholls[10] who have shown a connection between resonant interactions between Fourier modes and the multiplicity of solutions to the nonlinear problem. They used a surface formulation of Zakharov coupled with the Lyapunov–Schmidt procedure from bifurcation theory. The bifurcation points are determined by the solutions $(\mathbf{c},\mathbf{K})$ of the dispersion relation: $\Lambda_T(\mathbf{c},\mathbf{K})=(g+T\mathbf{K}^2)|\mathbf{K}|\tanh(h|\mathbf{K}|)-(\mathbf{c}\cdot\mathbf{K})^2=0$. For a fixed wave vector $\mathbf{K_1}\in\Gamma'$ (the conjugate to the lattice Γ of the spatial periods), the equation $\Lambda_T(\mathbf{c},\mathbf{K_1})=0$ determines two parallel lines of solutions, consisting of a particular solution pair $\pm\mathbf{c_0}$ and all parameters $\mathbf{c}'\in R^2$ such that $(\mathbf{c}'\pm\mathbf{c_0})\perp\mathbf{K_1}$. Given any two independent wave vectors $\mathbf{K_1},\mathbf{K_2}\in\Gamma'$, it is always possible to find a phase velocity vector $\mathbf{c}$ such that $\Lambda_T(\mathbf{c},\mathbf{K_1})=0$ and $\Lambda_T(\mathbf{c},\mathbf{K_2})=0$. It may be that the relation $\Lambda_T(\mathbf{c},\mathbf{K_j})=0$ is satisfied by other wave numbers $\mathbf{K_3},\mathbf{K_4},\ldots,\mathbf{K_p}$, as well as for $\mathbf{K_1}$ and $\mathbf{K_2}$ although this situation is not generic. These situations correspond to cases of bifurcation points of higher multiplicity, which are cases of resonance. This phenomenon is potentially stronger without surface tension. The analysis made by Craig and Nicholls[10] permitted "finite" resonance $(p<\infty)$ for $T>0$, while for $T=0$ they may encounter $p=\infty$ or, equally badly, $\Lambda_T(K_j,c)\ll 1$ for infinitely many K_j. Despite the fact that the problem becomes less difficult, there are very few results in the case where surface tension is taken into account. We mention, in particular, Kimmoun[11] and Bridges *et al.*[12] who computed from a formal point of view small amplitude gravity capillary short-crested waves. Despite that a natural analog of the Wilton ripple should be expected in three dimensions and that should generate new types of solutions, this phenomenon has not been yet analyzed to our knowledge. The importance of developing an analysis valid in three dimensions was highlighted by Reeder and Shinbrot.[13] Using the linear solution of the problem they have shown that, for Bond numbers $(=1/\kappa)$ near 2, bifurcation and ripple phenomena occur just as in two dimensions.

The averaged Lagrangian method of Whitham has been used by Marchant and Roberts[14,15] to formulate the problem of short-crested waves arising from the nonlinear interaction between incident and reflected wavetrains in two cases. In one case, the incident wavetrain forms a circular caustic where the wave field considered varies in the radial direction but has no angular variation. In the second case, the reflection occurs from a wedge of arbitrary angle and the wave field considered varies in the angular direction but has no radial variation.

In this article we use the averaged Lagrangian method of Whitham to the formulation of the classical problem of short-crested waves in the presence of gravity with and without surface tension. This formulation is applied in Sec. II to yield a set of nonlinear algebraic equations which is solved by Newton's method. The numerical procedure is described in Sec. III. Numerical solutions corresponding to three-dimensional Wilton ripples are presented in Sec. IV. The case of zero surface tension is considered in Sec. V, in particular, by computing the solutions corresponding to the strongest resonance (2, 6). The behavior of the method very near the limiting two-dimensional cases, the progressive stokes wave and the standing wave, is analyzed in Sec. VI. The case of small surface tension is handled in Sec. VII.

II. DERIVATION OF THE EQUATIONS

A. Preliminaries

This paper deals with short-crested water wave field which results from the nonlinear interaction of two periodic wavetrains of equal amplitude and frequency and nonzero angle of interaction. We consider the special case which occurs when a wavetrain of wavelength λ is obliquely incident on a vertical wall and is perfectly reflected (Fig. 1). The resulting wavetrain is three dimensional and propagates with constant speed c along the wall. At any point, the wave motion is still periodic in time as well as being periodic in the direction of propagation and in the transverse direction. A Cartesian coordinate system $\Re(o,x,y,z)$ is adopted with the x- and y-axes located on the still-water plane and the z-axis pointing vertically upward. The wave is assumed to propagate in the x-direction without change of shape. We assume

that the flow is irrotational and the fluid is perfect, of unit density and subject to the forces of gravity and surface tension.

Let the wavelength in the x-direction be $\lambda_x=\lambda/\sin\theta$ and the wavelength in the y-direction be $\lambda_y=\lambda/\cos\theta$. All the variables and the equations will be written in dimensionless form in which $K^{-1}=\lambda/2\pi$ and $(gK)^{-1/2}$ will be the length and time of reference. It is computationally convenient to use the frame of reference $\mathfrak{R}'(O,X,Y,Z)$, where

$$\begin{pmatrix} X \\ Y \\ Z \end{pmatrix} = \begin{pmatrix} px-\varpi t \\ qy \\ z \end{pmatrix}, \tag{1}$$

and in which the short-crested wave is steady with period 2π in X and Y. Here ϖ is the nondimensional frequency and p and q are the nondimensional X and Y direction wavenumbers, respectively, defined by

$$p=\sin\theta \quad \text{and} \quad q=\cos\theta. \tag{2}$$

For simplicity, only deep water is considered for which the nondimensional Lagrangian as proposed by Crapper[16] is

$$L=\int_{-\infty}^{\eta}\left[-\varpi\frac{\partial\Phi}{\partial X}+\frac{1}{2}(\vec{\nabla}\Phi)^2\right]dZ+\frac{1}{2}\eta^2 + \kappa[\sqrt{1+(\vec{\nabla}\eta)^2}-1], \tag{3}$$

where Φ is the nondimensional velocity potential, $Z=\eta(X,Y)$ is the equation of the free surface, and

$$\vec{\nabla}=\left(p\frac{\partial}{\partial X},q\frac{\partial}{\partial Y},\frac{\partial}{\partial Z}\right).$$

We seek expressions for $\Phi(X,Y,Z)$ and $\eta(X,Y)$ that are doubly periodic functions of the transformed horizontal coordinates. A general representation is

$$\Phi(X,Y,Z)=\sum_{m=1}^{\infty}\sum_{n=0}^{\infty}b_{mn}e^{\alpha_{mn}Z}\chi^{mn}(X,Y), \tag{4a}$$

$$\eta(X,Y)=\sum_{m=0}^{\infty}\sum_{n=0}^{\infty}\Delta_{m0}\Delta_{n0}a_{mn}\cos mX\cos nY, \tag{4b}$$

where

$$\chi^{mn}(X,Y)=\sin mX\cos nY \tag{5}$$

is introduced for notational convenience to calculate the kinetic energy and

$$\Delta_{j0}=1-\tfrac{1}{2}\delta_{j0}.$$

Here δ_{j0} is the Kronecker symbol and

$$\alpha_{mn}^2=p^2m^2+q^2n^2. \tag{6}$$

According to Whitham's method we define the averaged Lagrangian over a rectangular period, as proposed by Crapper,[16] to be

$$\bar{L}=\frac{1}{4\pi^2}\int_0^{2\pi}\int_0^{2\pi}\left\{\int_{-\infty}^{\eta}\left[-\varpi\frac{\partial\Phi}{\partial X}+\frac{1}{2}(\vec{\nabla}\Phi)^2\right]dZ+\frac{1}{2}\eta^2 + \kappa(\sqrt{1+(\vec{\nabla}\eta)^2}-1)\right\}dXdY. \tag{7}$$

Substituting expansions (4a) and (4b) into (7), the averaged Lagrangian $\bar{L}$ is obtained as a function of the unknown coefficients a_{mn} and b_{mn}. The explicit calculation of $\bar{L}$ is given in Appendix A where the averaged Lagrangian is expressed in the following way:

$$\bar{L}=\frac{1}{32}\sum_{m=1}^{\infty}\sum_{n=0}^{\infty}\sum_{k=1}^{\infty}\sum_{l=0}^{\infty}\frac{b_{mn}b_{kl}}{\alpha_{mn}+\alpha_{kl}}[\Omega^{mnkl}]^t[\Theta^{mnkl}] + \frac{\kappa}{4}(R_{00}-4)+\frac{1}{8}\sum_{m=0}^{\infty}\sum_{n=0}^{\infty}\Delta_{m0}\Delta_{n0}a_{mn}^2 - \frac{1}{4}\varpi\sum_{m=0}^{\infty}\sum_{n=0}^{\infty}m\frac{b_{mn}}{\alpha_{mn}}\omega_{mn}^{mn}. \tag{8}$$

The quantities ω_{mn}^{mn}, $R_{00}[\theta^{mnkl}]$, and $[\Omega^{mnkl}]$ are defined in Appendix A. Since $\bar{L}$ is independent of time, the variational equations to be solved are, according to Whitham's theory,

$$\frac{\partial\bar{L}}{\partial a_{rs}}=0, \tag{9a}$$

$$\frac{\partial\bar{L}}{\partial b_{rs}}=0. \tag{9b}$$

Applying Eqs. (9a) and (9b) to the averaged Lagrangian (8) yields the following set of nonlinear algebraic equations:

$$\frac{1}{32}\sum_{m=1}^{\infty}\sum_{n=0}^{\infty}\sum_{k=1}^{\infty}\sum_{l=0}^{\infty}\frac{b_{mn}b_{kl}}{\alpha_{mn}+\alpha_{kl}}[\bar{\Omega}_{rs}^{mnkl}]^t[\Theta^{mnkl}]+\frac{1}{4}\Delta_{r0}\Delta_{s0}a_{rs} + \frac{\kappa}{16}\sum_{m=0}^{\infty}\sum_{n=0}^{\infty}a_{mn}|\bar{T}_{mnrs}|^t|\vartheta_{mnrs}| - \frac{\varpi}{16}\Delta_{r0}\Delta_{s0}\sum_{m=0}^{\infty}\sum_{n=0}^{\infty}mb_{mn}\bar{\omega}_{mnrs}=0, \tag{10a}$$

$$\frac{1}{16}\sum_{m=1}^{\infty}\sum_{n=0}^{\infty}\frac{b_{mn}}{\alpha_{mn}+\alpha_{rs}}[\Omega^{mnrs}]^t[\Theta^{mnrs}]-\frac{\varpi}{4}\frac{r}{\alpha_{rs}}\omega_{rs}^{rs}=0, \tag{10b}$$

where the quantities $\bar{\omega}_{mnrs}$, $|\bar{T}_{mnrs}|$, and $|\vartheta_{mnrs}|$ are defined in Appendix B, while $[\bar{\Omega}_{rs}^{mnkl}]$ stands for the tensor

$$[\bar{\Omega}_{rs}^{mnkl}]=\frac{\partial}{\partial a_{rs}}[\Omega^{mnkl}].$$

III. NUMERICAL PROCEDURE

The series in Eqs. (4a) and (4b) are truncated at N and the order N is chosen for truncating the other expansions and the series in Eqs. (10a) and (10b). The resulting system may be written as

$$\frac{1}{32}\sum_{m=1}^{N}\sum_{n=0}^{N}\sum_{k=1}^{N}\sum_{l=0}^{N}\frac{b_{mn}b_{kl}}{\alpha_{mn}+\alpha_{kl}}[\bar{\Omega}_{rs}^{mnkl}]^t[\Theta^{mnkl}]+\frac{1}{4}\Delta_{r0}\Delta_{s0}a_{rs}+\frac{\kappa}{16}\sum_{m=1}^{N}\sum_{n=0}^{N}a_{mn}|\bar{T}_{mnrs}|^t|\vartheta_{mnrs}|-\frac{\varpi}{16}\Delta_{r0}\Delta_{s0}\sum_{m=1}^{N}\sum_{n=0}^{N}mb_{mn}\bar{\omega}_{mnrs}=0, \tag{11a}$$

$$\frac{1}{16}\sum_{m=1}^{N}\sum_{n=0}^{N}\frac{b_{mn}}{\alpha_{mn}+\alpha_{rs}}[\Omega^{mnrs}]^t[\Theta^{mnrs}]-\frac{\varpi}{4}\frac{r}{\alpha_{rs}}\omega_{rs}^{rs}=0,\quad r,s=0,1,2,3,\ldots,N. \tag{11b}$$

The above equations are to be solved for the unknowns a_{mn}, b_{mn}, and ϖ by fixing the values of θ and the steepness which is defined as

$$\varepsilon=\eta(0,0)-\eta(\pi,0)=\sum_{m=0}^{N}\sum_{n=0}^{N}a_{2m+1,2n+1}. \tag{12}$$

Note that $a_{00}=0$, the mean surface level being at $Z=0$ and, owing to the triangular symmetry of a short-crested wave,

$$a_{mm}=b_{mn}=0 \quad \text{when} \quad m+n \ \text{is odd}.$$

The number of unknowns is then

$$\tilde{N}=N^2+\tfrac{3}{2}\mathrm{N} \quad \text{if } N \text{ is even},$$

$$\tilde{N}=N^2+\tfrac{3}{2}N-\tfrac{1}{2} \quad \text{if } N \text{ is odd}.$$

The system of Eqs. (11a), (11b), and (12) is solved by Newton's method with the angle θ and the steepness ε regarded as parameters. In order to determine the increments of the coefficients in Newton's method, it is necessary to calculate the Jacobian matrix from the following equations:

$$\frac{\partial^2\bar{L}}{\partial b_{uv}\,\partial b_{rs}}=\frac{1}{16}\frac{1}{\alpha_{uv}+\alpha_{rs}}[\Omega^{uvrs}]^t[\Theta^{uvrs}], \tag{13}$$

$$\frac{\partial^2\bar{L}}{\partial a_{uv}\,\partial b_{rs}}=\frac{1}{16}\sum_{m=1}^{N}\sum_{n=0}^{N}\frac{b_{mn}}{\alpha_{mn}+\alpha_{rs}}[\bar{\Omega}_{uv}^{mnrs}]^t[\Theta^{mnrs}]-\frac{\varpi}{16}r\Delta_{u0}\Delta_{v0}\bar{\omega}_{rsuv}^{rs}, \tag{14}$$

$$\frac{\partial^2 L}{\partial a_{uv}\,\partial a_{rs}}=\frac{1}{32}\sum_{m=1}^{N}\sum_{n=0}^{N}\sum_{k=1}^{N}\sum_{l=0}^{N}\frac{b_{mn}b_{kl}}{\alpha_{mn}+\alpha_{kl}}[\bar{\bar{\Omega}}_{rsuv}^{mnkl}]^t[\Theta^{mnkl}]+\frac{1}{4}\Delta_{r0}\Delta_{s0}\delta_{ru}\delta_{sv}+\frac{\kappa}{16}|\bar{T}_{uvrs}|^t|\vartheta_{uvrs}|+\frac{\kappa}{16}\sum_{m=1}^{\infty}\sum_{n=0}^{\infty}a_{mn}\{|\bar{\bar{T}}_{uv}^{mnrs}|^t\}|\vartheta_{mnrs}|-\frac{\varpi}{16}\Delta_{r0}\Delta_{s0}\Delta_{u0}\Delta_{v0}\sum_{m=1}^{N}\sum_{n=0}^{N}mb_{mn}\bar{\bar{\omega}}_{mnrsuv}^{mn}, \tag{15}$$

where

$$[\bar{\bar{\Omega}}_{rsuv}^{mnkl}]=\frac{\partial^2}{\partial a_{rs}\,\partial a_{uv}}[\Omega^{mnkl}],$$

$$|\bar{\bar{T}}_{uv}^{mnrs}|=\frac{\partial}{\partial a_{uv}}|\bar{T}_{mnrs}|.$$

The Fourier coefficients introduced for the purposes of the present method are computed using the fast Fourier transform (FFT) algorithm. The computational domain is rectangular, periodic in both directions, and discretized with constant steps $\Delta X=\Delta Y=2\pi/M$. M and N may be chosen with a weak constraint, i.e., $M>2N$, in order to avoid the aliasing phenomenon.

In addition to the computational efficiency of the FFT algorithm, one can improve the method in order to reduce substantially the amount of calculations. To do so, we have chosen to compute the coefficients ω_{rs}^{klmn} defined by the relation (A6) by using

$$\omega_{rs}^{klmn}=\frac{1}{4}\sum_{i=0}^{\infty}\sum_{j=0}^{\infty}\Delta_{i0}\Delta_{j0}\omega_{ij}^{mn}\times[\omega_{i-r,j-s}^{kl}+\omega_{i-r,j+s}^{kl}+\omega_{i+r,j-s}^{kl}+\omega_{i+r,j+s}^{kl}] \tag{16}$$

instead of applying the FFT to the function $e^{(\alpha_{mn}+\alpha_{kl})\eta(X,Y)}$. This expression is obtained by computing the product $e^{\alpha_{mn}\eta(X,Y)}e^{\alpha_{kl}\eta(X,Y)}$. Doing so saves a considerable amount of system memory and shortens the calculation time. One can also note that

$$\omega_{rs}^{klmn}=\omega_{rs}^{mnkl},$$

and therefore the computations can be reduced by nearly half.

The initial estimates for the Newton iteration are given for small amplitudes by the approximations obtained by Ioualalen[17] for gravity waves and the ones of Kimmoun *et al.*[18] for gravity-capillary waves.

IV. THREE-DIMENSIONAL WILTON RIPPLES

Kimmoun[11] performed a sixth-order solution to the problem of short-crested gravity-capillary waves in finite depth by using the classical perturbation method which assumes that some parameter ε appearing in the equations is small. The solutions are then expanded as

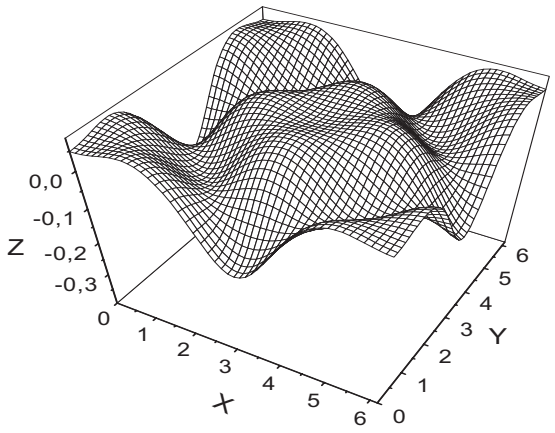

FIG. 2. Three-dimensional Wilton ripples of the type 1 for $\varepsilon=0.1$ and $\theta=\pi/4$.

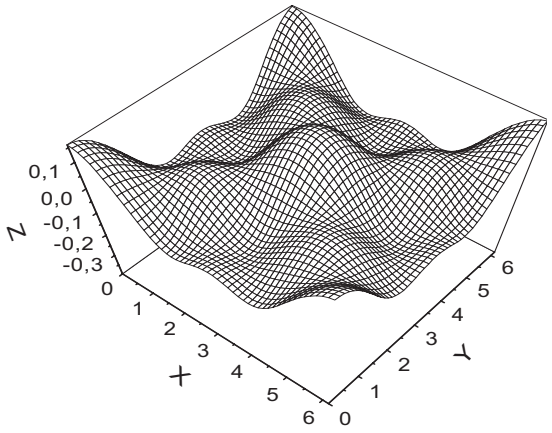

FIG. 3. Three-dimensional Wilton ripples of the type 2 for $\varepsilon=0.1$ and $\theta=\pi/4$.

$$\eta(X,Y)=\sum_R \varepsilon^R \eta_R(X,Y);$$

$$\eta_R(X,Y)=\sum_{j,k} a_{R,jk}\cos jX\cos kY, \tag{17}$$

$$\phi(X,Y)=\sum_R \varepsilon^R \phi_R(X,Y);$$

$$\phi_R(X,Y)=\sum_{j,k} b_{R,jk}\sin jX\cos kY\cosh \alpha_{jk}(Z+h), \tag{18}$$

where the subscript R indicates the order of the solution. He substituted these forms into the free surface boundary conditions which are then combined to give the following equation:

$$\kappa(p^2\phi_{R,ZXX}+q^2\phi_{R,ZYY})-\omega_0^2\phi_{R,XX}-\phi_{R,Z}=\text{rhs}, \tag{19}$$

with $\omega_0^2=(1+\kappa)\tanh(h)$ and h the depth. The right-hand side of Eq. (19) can contain terms of the form $\sin jX\cos kY\cosh \alpha_{jk}(Z+h)$ which are solutions of the associated homogeneous equation. These cases correspond to harmonic resonances and mean that the fundamental, $\sin X\cos Y\cosh(Z+h)$, excites the harmonic which propagates at the same phase speed. They occur if the parameters of the wave satisfy the relation

$$(1+\kappa\alpha_{j,k}^2)\alpha_{j,k}\tanh(\alpha_{j,k}h)-\omega_0^2 j^2=0. \tag{20}$$

In the parameter space this corresponds to the forbidden set introduced by Reeder and Shinbrot[2] and for which it is not possible to get a unique solution to the problem of short-crested capillary-gravity waves. In the case of deep water, Eq. (20) becomes

$$(1+\kappa\alpha_{j,k}^2)\alpha_{j,k}-(1+\kappa)j^2=0. \tag{21}$$

This is a generalization to short-crested waves of the relation giving the sets of parameters corresponding to Wilton ripples. We use our method to provide numerical evidence to the existence of this kind of three-dimensional solutions. Therefore, it is natural first to consider the resonances for which $j=k$ because κ will be equal to $1/k$ as in the two-dimensional case. For instance, for $j=k=2$, that is to say, $\kappa=1/2$, we obtain two types of solutions just as in two dimensions. Figures 2 and 3 show the shapes of these short-crested waves obtained with $\theta=\pi/4$. For small values of the wave steepness, the computations yield a wave of type 2 for $\kappa=1/2$. Wave of type 1 can be calculated from a solution computed with $\kappa=0.54$ varying progressively κ from 0.54 to 1/2 by step not exceeding few percents of the fixed value. Let us focus attention on the lines of intersection of the free surfaces plotted in Figs. 2 and 3 with the planes $X=2\pi$ or $Y=0$ (remind that the patterns are 2π-periodic in the both directions). Observe that these lines have the same shapes as the profiles of the two kinds of two-dimensional solutions found by Wilton and shown in Fig. 4. Furthermore, similar curves correspond to waves of the same type: the type 1 is capillarylike, that is to say, the wave speed decreases as the amplitude increases and the other is gravitylike with a speed that increases as the amplitude increases. This feature, known for two-dimensional Wilton ripples, is also observed for the three-dimensional corresponding cases as shown in Fig. 5. The case $\kappa=0.54$ is added to make comparisons with results of a neighboring nonresonant configuration. Now, the above mentioned similar characteristic features allow to come to the conclusion that the waves in Figs. 3 and 4 are

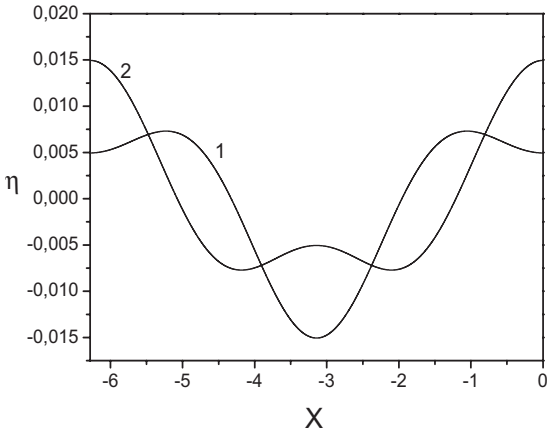

FIG. 4. The two profiles of two-dimensional Wilton ripples.

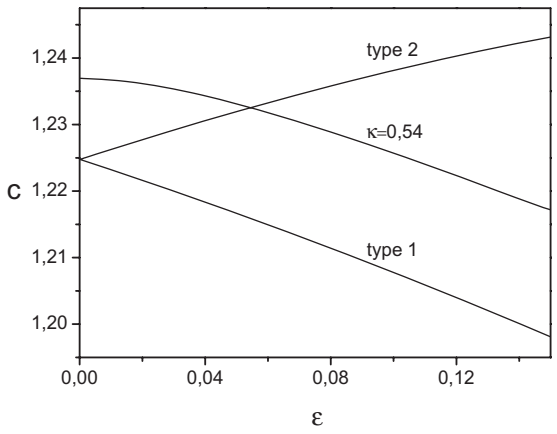

FIG. 5. Variation of wave speed with steepness for three-dimensional Wilton ripples and a nonresonant wave.

the three-dimensional analog of Wilton ripples. These similar features were also confirmed in the case corresponding to $\kappa=1/3$ [$j=k=3$ in Eq. (21)]. Plots of three-dimensional cases have been compared to those of their corresponding two-dimensional forms and, once again, the resemblance between the corresponding curves was remarkably close (Debiane[19]).

The more general case corresponding to $j\neq k$ in the relation (21) has been also considered. The resulting configuration gives rise to resonant solutions in which the basic element of symmetry is a rectangle of half-a-wavelength sides. Compared with the classical diamond pattern, it has lost the symmetry with respect to the diagonal of this rectangle. This feature is emphasized in Fig. 6 which shows a profile corresponding to a (4, 2) resonance.

V. SHORT-CRESTED GRAVITY WAVES

In contrast to the case that the surface tension is an included physical effect, the problem of pure short-crested gravity waves exhibits a strong phenomenon of small divisors which has implications for theoretical results of the problem. This problem dating from the work of Roberts[3] has received a lot of attention but it was found to be a tricky task.

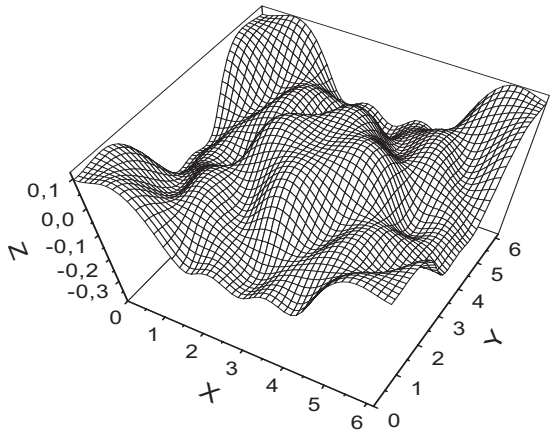

FIG. 6. Graph in perspective of short-crested capillary-gravity waves for $\varepsilon=0.1$ and $\theta=\pi/4$: case of (4,2) resonance.

TABLE I. Comparison between computed values of the phase velocity with the present method and those given by Ioualalen *et al.* (Ref. 9) and Cornier (Ref. 23). The numbers between brackets indicate the orders of truncation.

ε	Present method	Perturbation method (with use of the Shanks transform)	Numerical method
0.05	1.00044957 (5)	1.000 449 57 (5)	1.000 449 57 (5)
0.10	1.00180027 (7)	1.001 800 27 (9)	1.001 800 27 (5)
0.15	1.00405789 (8)	1.004 057 89(13)	1.004 057 89 (9)
0.195	1.00688445(13)	1.006 884 46(29)	1.006 884 45(13)
0.20	1.00723844(13)	1.007 238 44(25)	1.007 238 44(13)
0.25	1.01134021(13)	1.011 340 21(25)	1.011 340 21(13)
0.30	1.01639055(22)	1.016 390 55(25)	1.016 390 55(13)

Small divisors cause difficulties in the perturbation theory, and the convergence of the standard method is questionable due to the fact that the perturbation series have everywhere a zero radius of convergence. Roberts, who attributed the problem of small divisors to the phenomenon of harmonic resonance, has found that there are critical values of θ for which a division by zero occurs in the calculation of some coefficients at particular orders. The equation which relates these critical values to the (j,k)th resonant harmonic is

$$\cos^2\theta_c=\frac{(j^4-j^2)}{(k^2-j^2)}. \tag{22}$$

However, he found that for most of the cases the resonances occur at high orders and thus they should be dissipated through viscous damping. Thus, the truncated expansions at some order that leave out the resonant terms ought to provide a correct asymptotic approximation to the solutions of the problem. Furthermore, Roberts[3] used acceleration techniques such as the Padé approximants or the Shanks transform to obtain numerical convergence for finite amplitude waves. Recently, Ioualalen *et al.*[9] computed fully nonlinear short-crested waves using both a high-order perturbation expansion and a numerical method developed by Okamura.[20] In particular, the (2,6) resonance has been explored by taking θ equal to 53°, a value which is close to the critical angle $\theta_c=52.2388\ldots°$ given by Eq. (22) for the resonance (2,6). A detailed study of the properties of the solutions in a region about a singularity (a pole computed for ϖ) indicates that the problem admits multiple solutions: two branches matching each other through a turning point and one single branch. To check the accuracy of the present method, it is necessary to compare our results with those obtained by Ioualalen *et al.* A comparison between computed values of the phase velocity is presented in Table I. A good agreement is obtained for amplitudes up to and past the singularity. This method did not present singular behavior for critical angles given by Eq. (22), in particular, for the lowest order resonance (2,6) which seems to be one of the strongest. The corresponding solutions can be computed easily by either using appropriate initial conditions or by performing a bifurcation analysis. When the fourth-order approximations of Ioualalen[17] are used as initial estimate for Newton iterations, we obtain, at higher orders, the well-known symmetric diamond solution (Fig. 7).

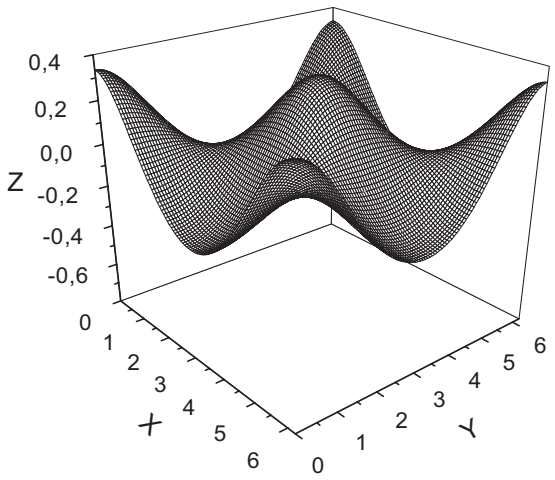

FIG. 7. Graph in perspective of nonresonant short-crested gravity waves for $\varepsilon=0.35$ and $\theta=\theta_c$ given by the relation (22) for $j=2$ and $k=6$.

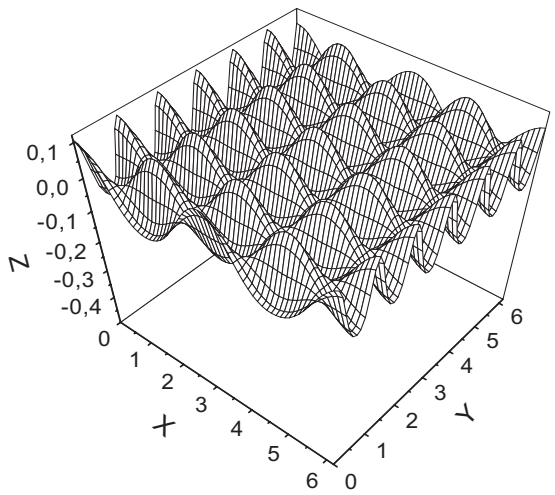

FIG. 8. Graph in perspective of regular resonant short-crested gravity wave for $\varepsilon=0.1$ and $\theta=\theta_c$ given by the relation (22) for $j=2$ and $k=6$ [case of the (2,6) resonance].

It seems that the latter, in which the harmonic (1,1) is dominant, can be regarded as a nonresonant case.

To solve the problem of three-dimensional gravity waves, Craig and Nicholls[21] have adopted a bifurcation theoretic approach in which they seek solutions near the quiescent state ($\Phi=\eta=0$ and any velocity c). They showed that the question of that traveling waves is a bifurcation problem with typical form of bifurcation branches which are two-dimensional surfaces as mentioned above in Sec. I. Nevertheless, the classical numerical continuation methods pose a difficulty and they suggest to map out portions of a bifurcation surface in (essentially) geodesic polar coordinates, or else to choose to follow certain distinguished curves in the bifurcation surfaces under consideration, using the more standard continuation method for bifurcation curves. To obtain the resonant solutions, we chose to adopt also a bifurcation approach, by using the parameter

$$Q=\eta(0,0). \tag{23}$$

This parameter appears to be more convenient than c because of its monotonic behavior. Fortunately, bifurcations occur about the trivial solution $(\eta,\Phi,c)=(0,0,c)$ where the solution branches are close enough to avoid the use of numerical continuation methods. Two types of (2,6) resonant waves have been obtained. The first is regular (uniform) and have wavelengths $\lambda_x=2\pi/2$ in the X-direction and $\lambda_y=2\pi/6$ in the Y-direction. This is because the coefficient a_{26} is the dominant coefficient in the solution set $\{a_{mn}\}$. The corresponding profile which is shown in Fig. 8 is similar to the one represented in Fig. 7 but the wavelengths are different. Figure 9 shows the profile of the second type of (2,6) resonant waves. The main feature to notice is that the wave is irregular with (2×6) crests of different heights in both horizontal directions. In this case, the coefficient a_{26} is of the same order as the coefficient a_{11} of the fundamental mode.

The method can be easily extended to the case where the indexes have a mixed parity. This is not in the present framework because of the fact that the triangular symmetry of cws excludes all mixed parity modes in the waves. However, several results have been obtained for these cases via our method, and we give in Fig. 10, as an example, a mixed-type solution where the wave is of type 1 in one component direction and type 2 in the other.

VI. THE TWO-DIMENSIONAL LIMITING CASES

The first two-dimensional limit is the standing wave and corresponds to angle $\theta=0°$, i.e., incident and reflected waves propagate in opposite directions. The other limit is the progressive Stokes wave for $\theta=\pi/2$, i.e., the two waves propagate in the same direction. Both of these limits have features of interest, but very little work has been done near the two-dimensional limits of short-crested waves. Roberts and Peregrine[4] have considered the limit as both incident and reflected waves are almost parallel. They found that harmonic resonances are due to the multilike structure of the solutions. Okamura[20] showed how short-crested waves match standing waves in deep water for $\theta\to0°$. It is found that the short-crested wave cannot be continued analytically

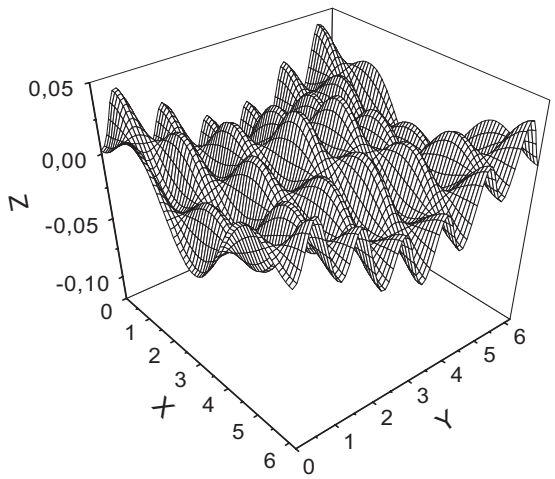

FIG. 9. Graph in perspective of nonregular resonant short-crested gravity wave for $\varepsilon=0.046$ and $\theta=\theta_c$ given by the relation (22) for $j=2$ and $k=6$ [case of the (2,6) resonance].

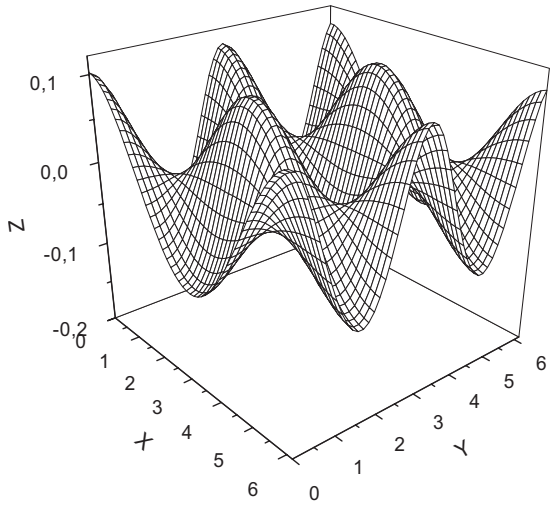

FIG. 10. Graph in perspective of a mixed type wave for $\varepsilon=0.1$: the wave is of type 1 in one component direction and type 2 in the other.

into the standing wave because of harmonic resonances. This work has been extended in Okamura *et al.*[22] to the case of standing waves on finite depth. In addition, the properties of the solutions have been discussed and a study on the superharmonic instabilities (resonant interactions) of short-crested waves was performed in the vicinity of the standing wave limit.

In the present study, we examine the behavior of short-crested waves very near their both two-dimensional limits, in the presence of harmonic resonance.

In a first case we took angle $\theta=10^{-4}$ and we computed easily solutions past the order of truncation 22 in the vicinity of the standing wave limit. At that angle, the wave is subject to (2, 4) and (3, 9) multiple harmonic resonances. This is in accordance with expectations since, following the resonance condition (22), when $k=j^2$ we find $\theta=0$ for all j; these harmonic resonances correspond to that occur in standing gravity waves. In Fig. 11 we report the branches of solutions b_{24} and b_{39} as a function of b_{11}. The dominant feature is that each coefficient is represented by two branches, (1) and (2), matching each other through a turning point (TP). Similar branches have been obtained for the case of finite depth by

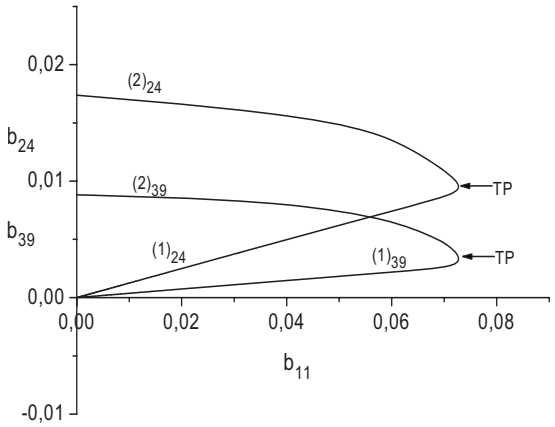

FIG. 11. Variation of the resonant coefficients b_{24} and b_{39} vs b_{11} for $\theta=10^{-4}$.

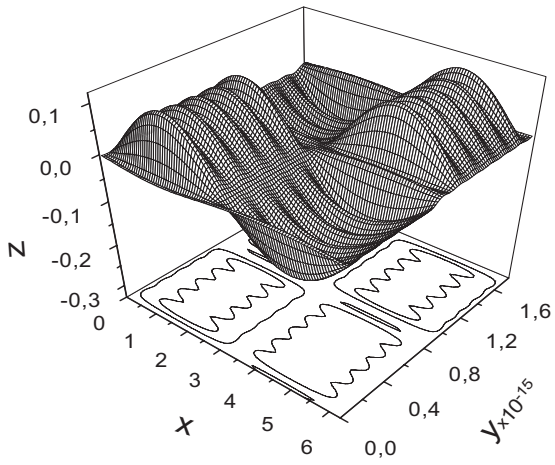

FIG. 12. Graph in perspective of long-crested gravity wave obtained for $\varepsilon=0.1$ and $\theta=\pi/2$. The y-coordinate is scaled with a factor of 10^{-15}.

Okamura *et al.*[22] for the resonant harmonic modes b_{35} and $b_{6,20}$ in the case of a nondimensional depth $d=0.62$ and $\theta=10^{-3}$. In contrast to the finite depth case, the resonant harmonic modes b_{24} and b_{39} can also be significant on branch (1) and the cross effects of b_{35} and $b_{6,20}$ branch solutions is not observed in our case.

In the second case, we consider the other limit which corresponds to the progressive Stokes wave for $\theta=\pi/2$. Two types of gravity waves have been obtained. Figures 12 and 13 show the shapes of these waves in the (x,y,z)-space. It may be useful to note that, in our numerical computations, π is the double precision value calculated by the computer with arccos (-1.0) and which is obtained to machine precision. Hence, this configuration corresponds to the closest to the two-dimensional progressive wave limit. Figure 12 represents the profile of the first type which is similar to those of the long-crested waves obtained to fourth-order accuracy by Roberts and Peregrine.[4] However, our profile exhibits ripples which have been examined to determine if they are not merely due to numerical error. The ripples do not disappear with an increase in the order of truncation up to the 25th order, even for very small values of steepness. Further tests

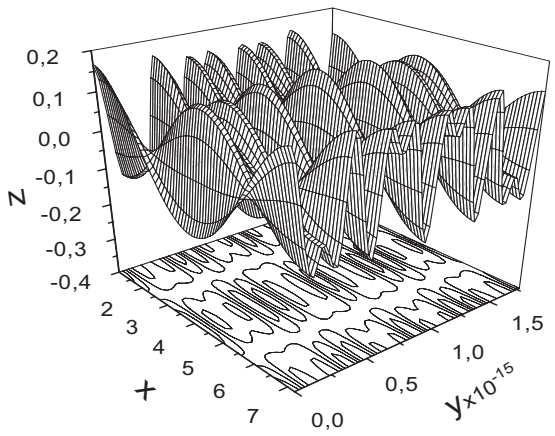

FIG. 13. Graph in perspective of resonant long-crested gravity wave obtained for $\varepsilon=0.16$ and $\theta=\pi/2$. The y-coordinate is scaled with a factor of 10^{-15}.

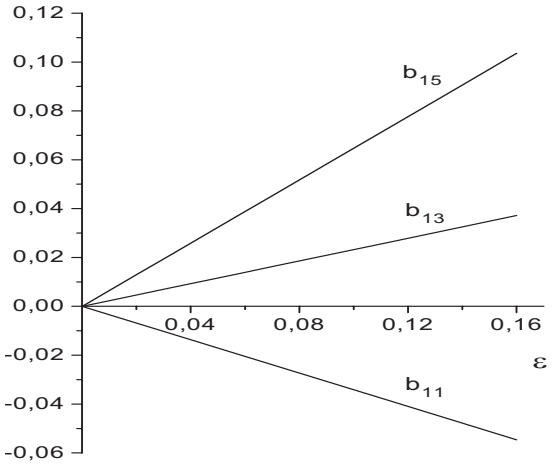

FIG. 14. Variation of the resonant coefficients b_{11}, b_{13}, and b_{15} with steepness for $\theta=\pi/2$.

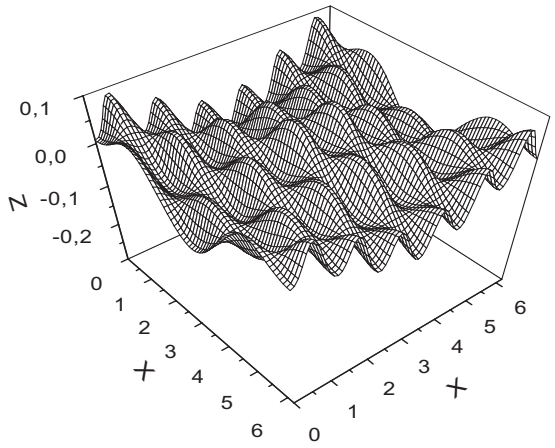

FIG. 16. Graph in perspective of nonregular resonant short-crested gravity wave for $\varepsilon=0.046\,26$, $\kappa=6\times10^{-6}$, and $\theta=52.303°$.

have been performed by keeping only the coefficients a_{mn} and b_{mn} with $m\leq 20$ and $n\leq 60$, since these coefficients are smaller than the machine precision when m is greater than 20. Once again, the ripples are apparent in the wave profile. Wave of this type can be calculated by varying progressively θ from a sufficiently small value to $\theta=\pi/2$. In this case, the most significant coefficients are b_{11}, b_{13}, and $b_{1,11}$ and the dominant mode is b_{11}. When the computations are performed using directly the value $\theta=\pi/2$, we obtain waves of the type represented in Fig. 13. These solutions are subject to multiple harmonic resonances where, in agreement with the resonance condition (22), many $(1, n)$ harmonic coefficients are the most significant and where dominant mode is b_{15}. Figure 14 represents the variation of the resonant coefficients b_{11}, b_{13}, and b_{15} with steepness for $\theta=\pi/2$.

Motivated by the efficiency of this method, we have examined the case of Wilton ripples for $\theta=\pi/2$. The obtained profile is shown in Fig. 15. It looks like gravity long-crested wave but it exhibits, in the direction of propagation, the characteristic shape of Wilton ripples of type 2.

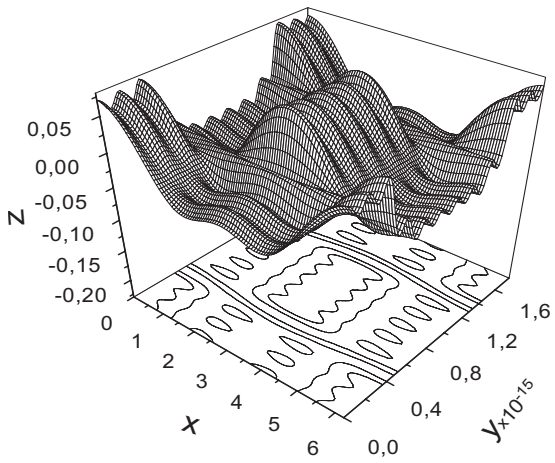

FIG. 15. Graph in perspective of Wilton ripples on long-crested wave obtained for $\varepsilon=0.05$, $\kappa=0.5$, and $\theta=\pi/2$. The y-coordinate is scaled with a factor of 10^{-15}.

VII. THE CASE OF SMALL SURFACE TENSION

Another case which is difficult to handle is the one of small surface tension which is the case in many usual situations. Our method works well also for this case. As an example, Fig. 16 shows the shape of the nonregular short-crested waves obtained with $\kappa=6\times10^{-6}$ and $\varepsilon=0.4626$. The comparison between Figs. 16 and 9 reveals that the two profiles are very similar.

VIII. CONCLUSION

Whitham's variational method has been applied successfully to the problem of resonant short-crested waves in which the appearance of small divisors causes the classical perturbation methods to fail. The problem was reduced to a system of nonlinear algebraic equations which was solved using Newton's method. It was shown that the method allows the computation of three-dimensional Wilton ripples and the resonant short-crested gravity waves. In particular, the method works well very near the limiting two-dimensional cases, the progressive stokes wave and the standing wave, and for the case of small surface tension.

APPENDIX A: CALCULATION OF THE AVERAGED LAGRANGIAN

This appendix describes details of the calculation of the averaged Lagrangian $\bar{L}$.

1. The kinetic energy

In the averaged Lagrangian function (7) given in the body of the paper, the contribution of the kinetic energy is

$$\overline{KE}=\frac{1}{8\pi^2}\int_0^{2\pi}\int_0^{2\pi}\int_{-\infty}^{\eta}(\vec{\nabla}\Phi)^2 dZdXdY. \tag{A1}$$

Substituting expansion (4a) into Eq. (A1), and integrating with respect to Z, the result can be written as

$$\overline{KE} = \frac{1}{8\pi^2}\sum_{m=1}^{\infty}\sum_{n=0}^{\infty}\sum_{k=1}^{\infty}\sum_{l=0}^{\infty}\frac{b_{mn}b_{kl}}{\alpha_{mn}+\alpha_{kl}} \times \int_0^{2\pi}\int_0^{2\pi} dXdY\{e^{(\alpha_{mn}+\alpha_{kl})\eta(X,Y)} \times\{\vec{\nabla}\chi^{mn}\vec{\nabla}\chi^{kl} + \alpha_{mn}\alpha_{kl}\chi^{mn}\chi^{kl}\}\}. \quad \text{(A2)}$$

By noting that

$$\chi^{mn}\chi^{kl} = \tfrac{1}{4}[\cos(k-m)X\cos(l-n)Y - \cos(k+m) \times X\cos(l-n)Y + \cos(k-m)X\cos(l+n) \times Y - \cos(k+m)X\cos(l+n)Y], \quad \text{(A3)}$$

$$\vec{\nabla}\chi^{mn}\vec{\nabla}\chi^{kl} = \tfrac{1}{4}p^2mk[\cos(k-m)X\cos(l-n)Y + \cos(k+m)X\cos(l-n)Y + \cos(k-m)X\cos(l+n)Y + \cos(k+m) \times X\cos(l+n)Y] + \tfrac{1}{4}q^2nl[\cos(k-m)X\cos(l-n)Y - \cos(k+m)X\cos(l-n)Y - \cos(k-m)X\cos(l+n) \times Y + \cos(k+m)X\cos(l+n)Y], \quad \text{(A4)}$$

we rewrite the kinetic energy as

$$\overline{KE} = \frac{1}{32\pi^2}\sum_{m=1}^{\infty}\sum_{n=0}^{\infty}\sum_{k=1}^{\infty}\sum_{l=0}^{\infty}\frac{b_{mn}b_{kl}}{\alpha_{mn}+\alpha_{kl}}\int_0^{2\pi}\int_0^{2\pi} e^{(\alpha_{mn}+\alpha_{kl})\eta(X,Y)}\{\cos(k-m)X\cos(l-n)Y[p^2mk + q^2nl + \alpha_{mn}\alpha_{kl}] + \cos(k-m)X\cos(l+n)Y[p^2mk - q^2nl + \alpha_{mn}\alpha_{kl}] + \cos(k+m)X\cos(l-n)Y[p^2mk - q^2nl - \alpha_{mn}\alpha_{kl}] + \cos(k+m)X\cos(l+n)Y[p^2mk + q^2nl - \alpha_{mn}\alpha_{kl}]\}dXdY. \quad \text{(A5)}$$

It is helpful to use the following Fourier expansion:

$$e^{(\alpha_{mn}+\alpha_{kl})\eta(X,Y)} = \sum_{u=0}^{\infty}\sum_{v=0}^{\infty}\Delta_{u0}\Delta_{v0}\omega_{uv}^{mnkl}\cos uX\cos vY \quad \text{(A6)}$$

where the coefficients ω_{uv}^{mnkl} can be easily computed by using the relation (16) given in the body of the paper. In doing so, it is straightforward to obtain the result of Eq. (A5) under the form

$$\overline{KE} = \frac{1}{32}\sum_{m=1}^{\infty}\sum_{n=0}^{\infty}\sum_{k=1}^{\infty}\sum_{l=0}^{\infty}\frac{b_{mn}b_{kl}}{\alpha_{mn}+\alpha_{kl}} \times[\omega_{k-m,l-n}^{mnkl}(p^2mk + q^2nl + \alpha_{mn}\alpha_{kl}) + \omega_{k+m,l-n}^{mnkl}(p^2mk - q^2nl - \alpha_{mn}\alpha_{kl}) + \omega_{k-m,l+n}^{mnkl}(p^2mk - q^2nl + \alpha_{mn}\alpha_{kl}) + \omega_{k+m,l+n}^{mnkl}(p^2mk + q^2nl - \alpha_{mn}\alpha_{kl})], \quad \text{(A7)}$$

which can be expressed in a compact form by

$$\overline{KE} = \frac{1}{32}\sum_{m=1}^{\infty}\sum_{n=0}^{\infty}\sum_{k=1}^{\infty}\sum_{l=0}^{\infty}\frac{b_{mn}b_{kl}}{\alpha_{mn}+\alpha_{kl}}[\Omega^{mnkl}]^t[\Theta^{mnkl}], \quad \text{(A8)}$$

where $[\Omega_{mnkl}]$ and $[\Theta_{mnkl}]$ are column matrices given by

$$[\Theta^{mnkl}] = \begin{bmatrix} p^2mk + q^2nl + \alpha_{mn}\alpha_{kl} \\ p^2mk - q^2nl + \alpha_{mn}\alpha_{kl} \\ p^2mk - q^2nl - \alpha_{mn}\alpha_{kl} \\ p^2mk + q^2nl - \alpha_{mn}\alpha_{kl} \end{bmatrix}, \quad \text{(A9)}$$

$$[\Omega^{mnkl}] = \begin{bmatrix} \omega_{k-m,l-n}^{mnkl} \\ \omega_{k-m,l+n}^{mnkl} \\ \omega_{k+m,l-n}^{mnkl} \\ \omega_{k+m,l+n}^{mnkl} \end{bmatrix}. \quad \text{(A10)}$$

2. The potential energy

In the right-hand side of Eq. (7), the averaged potential energy $\bar{V}_g$ due to gravity only is defined as

$$\bar{V}_g = \frac{1}{4\pi^2}\int_0^{2\pi}\int_0^{2\pi}\left[\frac{1}{2}\eta^2\right]dXdY = \frac{1}{8}\sum_{m=0}^{\infty}\sum_{n=0}^{\infty}\Delta_{m0}\Delta_{n0}a_{mn}^2. \quad \text{(A11)}$$

On the other hand, for the term of the averaged capillary energy defined by

$$\bar{V}_\tau = \frac{\kappa}{4\pi^2}\int_0^{2\pi}\int_0^{2\pi}\left[\sqrt{1+p^2\left(\frac{\partial\eta}{\partial X}\right)^2 + q^2\left(\frac{\partial\eta}{\partial Y}\right)^2} - 1\right] \times dXdY, \quad \text{(A12)}$$

we introduce the following Fourier expansion:

$$\sqrt{1+p^2\left(\frac{\partial\eta}{\partial X}\right)^2+q^2\left(\frac{\partial\eta}{\partial Y}\right)^2}=\sum_{m=0}^{\infty}\sum_{n=0}^{\infty}\Delta_{m0}\Delta_{n0}R_{mn}\times\cos mX\cos nY \tag{A13}$$

that enables us to compute easily the integral, and one gets

$$\bar{V}_\tau=\frac{\kappa}{4}(R_{00}-4), \tag{A14}$$

R_{00} is computed using the FFT algorithm.

3. The averaged temporal rate of variation of the velocity potential

The remaining term represents the temporal rate of variation of the potential which reads

$$\bar{\Phi}_t=\frac{1}{4\pi^2}\int_0^{2\pi}\int_0^{2\pi}\int_{-\infty}^{\eta}-\varpi\Phi_X dZdXdY. \tag{A15}$$

Using the expansion (4a) and after integration with respect to Z, one obtains

$$\bar{\Phi}_t=-\frac{\varpi}{4\pi^2}\sum_{m=1}^{\infty}\sum_{n=0}^{\infty}m\frac{b_{mn}}{\alpha_{mn}}\times\int_0^{2\pi}\int_0^{2\pi}e^{\alpha_{mn}\eta}\cos mX\cos nYdXdY. \tag{A16}$$

The integral of the right-hand side suggests to use the coefficients of Fourier's expansion of the function

$$e^{\alpha_{mn}\eta(X,Y)}=\sum_{i=0}^{\infty}\sum_{j=0}^{\infty}\Delta_{i0}\Delta_{j0}\omega_{ij}^{mn}\cos iX\cos jY, \tag{A17}$$

where

$$\omega_{ij}^{mn}=\frac{1}{\pi^2}\int_0^{2\pi}\int_0^{2\pi}e^{\alpha_{mn}\eta}\cos iX\cos jYdXdY. \tag{A18}$$

In doing so, the integral result is easily found as

$$\bar{\Phi}_t=-\frac{1}{4}\varpi\sum_{m=0}^{\infty}\sum_{n=0}^{\infty}m\frac{b_{mn}}{\alpha_{mn}}\omega_{mn}^{mn}. \tag{A19}$$

Using expressions (A8), (A11), (A14), and (A19), the averaged Lagrangian function (7) is obtained as a function of the coefficients and can be written in the form

$$\bar{L}=\frac{1}{32}\sum_{m=1}^{\infty}\sum_{n=0}^{\infty}\sum_{k=1}^{\infty}\sum_{l=0}^{\infty}\frac{b_{mn}b_{kl}}{\alpha_{mn}+\alpha_{kl}}[\Omega^{mnkl}]^t[\Theta^{mnkl}]+\frac{\kappa}{4}(R_{00}-4)+\frac{1}{8}\sum_{m=0}^{\infty}\sum_{n=0}^{\infty}\Delta_{m0}\Delta_{n0}a_{mn}^2-\frac{1}{4}\varpi\sum_{m=0}^{\infty}\sum_{n=0}^{\infty}m\frac{b_{mn}}{\alpha_{mn}}\omega_{mn}^{mn}. \tag{A20}$$

APPENDIX B: EXPRESSIONS OF SOME DERIVATIVES

This appendix gives expressions of some derivatives not reported in the body of the paper. They are useful to calculate the Jacobian matrix which is necessary to determine the increments of the coefficients in Newton's method. For more details see Debiane.[19]

$$\frac{\partial\omega_{ij}^{mn}}{\partial a_{rs}}=\frac{\Delta_{r0}\Delta_{s0}\alpha_{mn}}{4}\bar{\omega}_{ijrs}^{mn}, \tag{B1}$$

with

$$\bar{\omega}_{mnrs}=\omega_{r-m,s-n}^{mn}+\omega_{r-m,s+n}^{mn}+\omega_{r+m,s-n}^{mn}+\omega_{r+m,s+n}^{mn}, \tag{B2}$$

$$\frac{\partial^2\omega_{ij}^{mn}}{\partial a_{rs}\,\partial\, a_{uv}}=\frac{\alpha_{mn}}{4}\Delta_{r0}\Delta_{s0}\Delta_{u0}\Delta_{v0}\bar{\bar{\omega}}_{ijrsuv}^{mn},$$

with

$$\bar{\bar{\omega}}_{ijrsuv}^{mn}=\frac{1}{\Delta_{r-u,0}\Delta_{s-v,0}}\frac{\partial\omega_{ij}^{mn}}{\partial a_{r-u,s-v}}+\frac{1}{\Delta_{r-u,0}\Delta_{s+v,0}}\frac{\partial\omega_{ij}^{mn}}{\partial a_{r-u,s+v}}+\frac{1}{\Delta_{r+u,0}\Delta_{s-v,0}}\frac{\partial\omega_{ij}^{mn}}{\partial a_{r+u,s-v}}+\frac{1}{\Delta_{r+u,0}\Delta_{s+v,0}}\frac{\partial\omega_{ij}^{mn}}{\partial a_{r+u,s+v}}, \tag{B3}$$

$$\frac{\partial R_{00}}{\partial a_{rs}}=\frac{1}{4}\sum_{m=0}^{\infty}\sum_{n=0}^{\infty}a_{mn}|\bar{T}_{mnrs}|^t|\vartheta_{mnrs}|, \tag{B4}$$

where $[\vartheta_{mnrs}]$ and $[\bar{T}_{mnrs}]$ are column matrices given by

$$[\vartheta_{mnrs}]=\begin{bmatrix}\Delta_{n0}\Delta_{s0}p^2mr+\Delta_{m0}\Delta_{r0}q^2ns\\ \Delta_{n0}\Delta_{s0}p^2mr-\Delta_{m0}\Delta_{r0}q^2ns\\ -\Delta_{n0}\Delta_{s0}p^2mr+\Delta_{m0}\Delta_{r0}q^2ns\\ -\Delta_{n0}\Delta_{s0}p^2mr-\Delta_{m0}\Delta_{r0}q^2ns\end{bmatrix}, \tag{B5}$$

$$[\bar{T}_{mnrs}]=\begin{bmatrix}T_{r-m,s-n}\\ T_{r-m,s+n}\\ T_{r+m,s-n}\\ T_{r+m,s+n}\end{bmatrix}. \tag{B6}$$

T_{mn} being Fourier coefficients defined by

$$\frac{1}{\sqrt{1+(\vec{\bar{\nabla}}\eta)^2}}=\sum_{m=0}^{\infty}\sum_{n=0}^{\infty}\Delta_{m0}\Delta_{n0}T_{mn}\cos mX\cos nY, \tag{B7}$$

$$\frac{\partial T_{ij}}{\partial a_{uv}}=-\frac{1}{16}\sum_{m=0}^{\infty}\sum_{n=0}^{\infty}a_{mn}|\Gamma_{mnuv}^{ij}|^t|\vartheta_{mnuv}|, \tag{B8}$$

where $[\Gamma_{mnuv}^{ij}]$ is a column matrix given by

$$|\Gamma^{ij}_{rsuv}| = \begin{vmatrix} P_{|u-m|+i,|v-n|+j} + P_{|u-m|+i,|v-n|-j} + P_{|u-m|-i,|v-n|+j} + P_{|u-m|-i,|v-n|-j} \\ P_{|u-m|+i,v+n+j} + P_{|u-m|+i,v+n-j} + P_{|u-m|-i,v+n+j} + P_{|u-m|-i,v+n-j} \\ P_{u+m+i,|v-n|+j} + P_{u+m+i,|v-n|-j} + P_{u+m-i,|v-n|+j} + P_{u+m-i,|v-n|-j} \\ P_{u+m+i,v+n+j} + P_{u+m+i,v+n-j} + P_{u+m-i,v+n+j} + P_{u+m-i,v+n-j} \end{vmatrix}. \quad \text{(B9)}$$

P_{kl} are Fourier coefficients defined by

$$\frac{1}{[1+(\vec{\nabla}\eta)^2]^{3/2}} = \sum_{k=0}^{\infty}\sum_{n=0}^{\infty} \Delta_{k0}\Delta_{l0}P_{kl}\cos kX \cos lY. \quad \text{(B10)}$$

[1] J. R. Wilton, "On ripples," Philos. Mag. **29**, 688 (1915).
[2] J. Reeder and M. Shinbrot, "Three-dimensional, nonlinear wave interaction in water of constant depth," Nonlinear Anal. Theory, Methods Appl. **5**, 303 (1981).
[3] A. J. Roberts, "Highly nonlinear short-crested water waves," J. Fluid Mech. **135**, 323 (1983).
[4] A. J. Roberts and D. H. Peregrine, "Notes on long-crested waves," J. Fluid Mech. **135**, 301 (1983).
[5] T. R. Marchant and A. J. Roberts, "Properties of short-crested waves in water of finite depth," J. Aust. Math. Soc. Ser. B, Appl. Math. **29**, 103 (1987).
[6] G. Ioss and P. Plotnikov, "Small divisor problem in the theory of three-dimensional water gravity waves," Mem. Am. Math. Soc. (in press).
[7] M. Ioualalen and C. Kharif, "Stability of three dimensional progressive gravity waves on deep water to superharmonic disturbances," Eur. J. Mech. B/Fluids **12**, 401 (1993).
[8] M. Ioualalen and M. Okamura, "Structure of the instability associated with harmonic resonance of short-crested waves," J. Phys. Oceanogr. **32**, 1331 (2002).
[9] M. Ioualalen, M. Okamura, S. Cornier, C. Kharif, and A. J. Roberts, "Computation of short-crested deepwater waves," J. Waterway, Port, Coastal, Ocean Eng. **132**, 157 (2006).
[10] W. Craig and D. P. Nicholls, "Travelling two and three dimensional capillary gravity water waves," SIAM J. Math. Anal. **32**, 323 (2000).
[11] O. Kimmoun, "Etude théorique et expérimentale des champs de vagues à courtes crêtes," P.D. thesis, Université de la Méditerranée, 1997.
[12] T. J. Bridges, F. Dias, and D. Menasce, "Steady three-dimensional water-wave patterns on a finite-depth fluid," J. Fluid Mech. **436**, 145 (2001).
[13] J. Reeder and M. Shinbrot, "On Wilton ripples I: Formal derivation," Wave Motion **3**, 115 (1981b).
[14] T. R. Marchant and A. J. Roberts, "A variational approach to the problem of deep water waves forming a circular caustic," J. Fluid Mech. **194**, 581 (1988).
[15] T. R. Marchant and A. J. Roberts, "Reflection of nonlinear deep-water waves incident onto a wedge of arbitrary angle," J. Aust. Math. Soc. Ser. B, Appl. Math. **32**, 61 (1990).
[16] G. D. Crapper, "Energy and momentum integrals for progressive capillary-gravity waves," J. Fluid Mech. **94**, 13 (1979).
[17] M. Ioualalen, "Fourth order approximation of short-crested waves," C. R. Acad. Sci., Ser. II: Mec., Phys., Chim., Sci. Terre Univers **316**, 1193 (1993).
[18] O. Kimmoun, H. Branger, and C. Kharif, "On short-crested waves: Experimental and analytical investigations," Eur. J. Mech. B/Fluids **18**, 889 (1999).
[19] M. Debiane, "Contribution à l'étude des ondes de surface," Doctorat d'état, Université des Sciences et de la Technologie Houari Boumediène Algiers, Algeria, 2005.
[20] M. Okamura, "Notes on short-crested waves in deep water," J. Phys. Soc. Jpn. **65**, 2841 (1996).
[21] W. Craig and D. P. Nicholls, "Traveling gravity water waves in two and three dimensions," Eur. J. Mech. B/Fluids **21**, 615 (2002).
[22] M. Okamura, M. Ioualalen, and C. Kharif, "Standing waves on water of uniform depth: On their resonances and matching with short-crested waves," J. Fluid Mech. **495**, 145 (2003).
[23] S. Cornier, "Détermination d'ondes de surface de gravité tridimensionnelles à courtes crêtes résonantes par deux méthodes de calcul et propriétés," Rapport de stage de Diplôme d'Etudes Approfondies, Université Aix-Marseille II et Université de Toulon et du Var, France, 2004.